

# Energy Storage Performance of Hydrogen Fuel Cells Operating in a Marine Salt Spray Environment using Experimental Evaluation

**Xiaofei Wen, Dandan Zhu**

Donghai Laboratory

Zhoushan 316021, China

**Anna Hnydiuk-Stefan**

Department of Power Engineering Management

Opole University of Technology

Opole 45758, Poland

**Zhenjun Ma**

Sustainable Buildings Research Centre

University of Wollongong

NSW 2522, Australia

**Grzegorz Królczyk, Z Li**

Faculty of Mechanical Engineering

Opole University of Technology

Opole 45758, Poland

Corresponding Author: z.li@po.edu.pl

**Abstract:** In a marine salt spray environment, sodium chloride poisoning will significantly deteriorate the performance of the hydrogen fuel cells; for example, proton exchange membrane fuel cells (PEMFCs). Currently, the degradation mechanisms of the PEMFC caused by the sodium chloride poisoning are often evaluated by the pollution of the F ions;

however, the pollution of the sodium chloride in the membrane electrodes is seldomly inspected. In this avail, this work experimentally explores the influence of the sodium chloride pollution on the PEMFC performance in the marine salt spray environment by analyzing the concentration diffusion characteristics of the sodium chloride in the PEMFC membrane electrodes. Firstly, a set of experiments were carried out to determine the distribution of the sodium chloride components in the membrane electrodes, where five different salt spray environments (i.e., 100 mg/L, 200 mg/L, 300 mg/L, 400 mg/L, and 500 mg/L of the salt component, respectively) were used/employed to analyze the concentration diffusion characteristics of the sodium chloride. Then, the obtained samples were microscopically characterized and elementally analyzed by the field emission scanning electron microscopy (FESEM) and the energy spectrometry. Subsequently, a least squares-based model was proposed to predict the diffusion rate of the contaminating ions in the membrane electrodes. Lastly, the pollution of the sodium chloride was evaluated/assessed to reveal the performance degradation of the PEMFCs. The experimental results demonstrated that (1) the sodium chloride fraction existed as crystals or ions in the membrane electrodes in the marine salt spray environment; (2) the sodium chloride poisoning was founded in the proton exchange membrane in the form of sodium ions; (3) and the sodium-to-chloride ratio was proportional to the contamination time and the salt spray in the proton exchange membrane.

**Keywords:** Hydrogen fuel cells; proton exchange membrane fuel cell; membrane electrode; salt spray test

## 1. Introduction

The proton exchange membrane fuel cell (PEMFCs) ~~is a typical type of hydrogen fuel cells and~~ has been an emergent alternative to fossil fuels in the marine power systems because of high practicability and low emissions and environmental pollution. However, in a marine salt-spray environment, the sodium and chloride concentrations are much higher than these in the inland areas, which results in that the sodium chloride poisoning frequently occurs in the PEMFCs to cause an irreversible decay on the PEMFCs performance [1, 2]. The term "sodium chloride poisoning" was introduced by Mikkola [3], who found that the sodium chloride can damage the catalyst in the PEMFCs and lead to degradation of battery performance. Unnikrishnan et al. [4] stated that the

chlorine contamination can cause performance loss on the battery anode and cathode by 94 % and 82 %, respectively. Therefore, it is critical to study the mechanism of sodium chloride poisoning in marine salt spray environment to prevent battery degradation.

The durability of the proton exchange membrane is one of the most important indicators of cell performance, and proton exchange membrane operation is subject to contamination from various materials in the cell stack, coolant, and fuel-side contaminants [5]. Impurities from the air side enter the cathode side of the PEMFC, where they dissolve in liquid water and penetrate the cathode side under a concentration gradient, causing degradation or failure of the cell during operation [6]. And for the sodium chlorine poisoning, when the chlorine enters the PEMFC the chlorine ions are adsorbed on the catalyst Pt surface, which may damage the catalyst. Literature review indicates that impurities have been found to degrade cell performance by affecting the  $H^+$  content and the active specific surface area of the catalytic layer [7] and the degree of contamination is usually evaluated in terms of the release rate of F ions, the atomic percentage and the migration rate of impurities. Recent progress suggests that the membrane cation contamination is an important cause of the battery degradation. For example, Wang et al. [7] investigated the degree of contamination of the membrane electrode components by immersion experiments in perionic solutions ( $Ca^{2+}$ ,  $Mg^{2+}$ ,  $Na^+$ ), studied the effect of the contaminated solution environment on the catalytic and gas diffusion layers, and found that the  $H^+$  in the proton exchange membrane was more contaminated by metal cations than the catalytic layer. Jie et al. [8] found that the presence of  $Na^+$  had a significant toxic effect on the Pt/C. In 2009, Strmcnik et al [9] proposed a cluster of non-covalent interactions between Pt and surface oxides on cations (containing  $Na^+$  ), leading to the occupation of Pt active sites in electrochemical reactions. Jayasayee et al [10] carried out a study on the relationship between  $Cl^-$  concentration and dissolution rate of PtNi alloy by energy dispersive X-ray spectroscopy( EDX) and inductively coupled plasma spectroscopy and determined that  $Cl^-$  enhanced the dissolution of Pt and Ni by monitoring the changes in the percentage of Pt and Ni atoms. Uddin et al. [11] analyzed the surface and cross-section of the gas diffusion layer of the cell membrane electrode and the cross-sectional morphology of the catalytic coating membrane (CCM) by Scanning electron microscopy (SEM) and energy dispersive X-ray spectroscopy (EDS), and the results showed that cations were not detected in the CCM, but the study indicated that chloride ions reduced the catalyst activity specific surface area.

87 Arruda T et al.[12]studied the competition of anion adsorption on the catalyst Pt surface by the spectra  
88 formed by XRD, EDX in a half-cell system. Mo et al. [13] analyzed the migration of corrosion product  
89 metal cations in PEMEC catalyst coating membranes with EDS images, showing that high levels of  
90 Fe cations in Nafion membranes occupied the water nanochannels in the membranes, reducing the  
91 proton transport efficiency in PEM. Gutleben et al. [14] showed that the degradation of Pt was caused  
92 by the electrochemical reaction of chloride in the vicinity of the membrane. The chemical degradation  
93 of the membrane is mainly due to the vulnerability of the SO<sub>3</sub>H, CF<sub>3</sub>, OCF<sub>2</sub> and CF groups on the  
94 side chains of the perfluoro sulfonic acid polymer to attack by (-OH) radicals and shedding, resulting  
95 in the destruction of the function and integrity of the proton exchange membrane [15, 16]. Hori et al.  
96 [17] studied the dissociation of F- from fluorine elements in membranes after immersion in a  
97 contaminated solution containing iron, along with the appearance of intermediate products in the  
98 membrane side chains. Zhang et al. [18] showed that the rate of fluorine ion release from membranes  
99 was linearly and positively correlated with the time of contamination. Kelly et al. [19] evaluated the  
100 degree of membrane contamination by determining the calculated ion uptake in membranes based on  
101 the concentration of cationic impurities and by energy dispersive X-ray analysis through the atomic  
102 percentage ratio. Inaba et al. [20] studied the rate of reaction between air and hydrogen at the fuel  
103 side to generate free radicals, the rate of release of fluorine ions by to compare the fast rate of  
104 generation of fluorine ions on the anode side and the cathode side. Liu et al [21] found by in situ  
105 detection method that the anode produced free radicals diffused to the cathode side through the  
106 concentration difference thus leading to the attenuation of the proton film. By in situ detection method,  
107 it was found that the anode produced free radicals diffused to the cathode side through the  
108 concentration difference thus leading to the decay of the proton film. Kienitz et al. [22] investigated  
109 the degradation of the performance of a proton exchange membrane fuel cell contaminated with  
110 foreign cations (Na<sup>+</sup>, Ca<sup>2+</sup> or metal ions) in a half-cell model by numerical simulations, and evaluated  
111 the contaminant and proton transport through diffusion and migration by comparing the rate of release  
112 of fluoride ions from the anode side and the cathode side. Xie et al. [23] evaluated the degree of  
113 contamination by observing the crack expansion of the membrane through electron micrographs and  
114 performed molecular simulations of weight loss and product emission rates as time to model the  
115 chemical contamination degradation and mechanical deformation of the membrane. Md Aman Uddin

et al. [24] investigated the effect of the gas diffusion layer (GDL) on cationic contamination of polymer electrolyte fuel cells (PEFCs) by soaking three membrane electrode assembly (MEA) structures in cationic ( $\text{Ca}^{2+}$ ) solution. The results showed that the hydrophobicity of GDL and microporous layer (MPL) was a barrier to the cationic solution reaching CCM.

In summary, ~~although existing literatures have indicated that the contamination of the membrane electrode components causes absolute PEMFC degradation, very limited work has been done to address the PEMFC degradation mechanisms in the marine salt spray environment.~~ for the PEMFC-powered ships, it is inevitable to investigate on the influence of the sodium chloride on the membrane electrodes and explore the PEMFC degradation mechanisms. ~~However, there is little work on this in existing literatures. little work has been done yet.~~ To this end, this study examines the effects of the diffusion rate and contamination of the sodium chloride in the membrane electrodes to explore the battery degradation in the marine salt-spray environment. The evaluation of the contamination degree provides a theoretical basis for addressing the adverse effects of impurity ions on the battery and implications for the development of battery contamination mitigation strategies in the marine salt-spray environment.

The remainder of this paper is organized as follows. Experimental test of the sodium chloride pollution on the PEMFC membrane electrodes in the marine salt-spray environment is carried out in Section 2. In Section 3, the experimental results are presented. The evaluation of the contamination level of  $\text{Na}^+$  in the membranes is performed in Section 4. Conclusions and future works are summarized in Section 5.

## 2. Experimental Materials and Results

### 2.1 Experiment Preparation

According to the operation of salt spray aerosol and the principle of salt spray generation, based on the conditions of the marine atmospheric environment parameters, the marine environment is simulated through the standard salt spray test chamber, where the salt spray particle size is between  $0.1\mu\text{m}$  and  $0.5\mu\text{m}$ , the salt spray concentration is between  $100\text{mg}/\text{m}^3$  and  $500\text{mg}/\text{m}^3$ , the temperature is between  $25^\circ\text{C}$  and  $45^\circ\text{C}$ , the humidity is between 85%RH and 95%RH, and the settling volume is between  $1\text{ml}/80\text{cm}^2/\text{h}$  and  $2\text{ml}/80\text{cm}^2/\text{h}$ . Accelerating test and natural atmospheric exposure test are carried out by loading the salt spray contents with different ratios, and refer to [25], the salt mist

145 content ranges between  $0.2\text{mg/m}^3$  and  $0.66\text{mg/m}^3$ . Fig. 1 manifests the experimental test procedure,  
146 where the gas phase test is carried out to evaluate the sodium and chloride contamination effect on  
147 the battery membrane electrodes. The experimental procedure is described as follows.[26-27].

148 (1) Prepare the experimental membrane electrodes. Firstly, a  $5\text{cm} \times 5\text{cm}$  membrane electrode is  
149 divided into five  $1\text{cm} \times 5\text{cm}$  membrane electrode samples. The mass of each sample is  
150 weighed with an analytical balance. Then each sample is put into a vacuum drying oven at  
151  $80^\circ\text{C}$  for 8 hours and baked until its mass is constant.

152 (2) Prepare the salt spray test solution. Firstly, dissolve the pure sodium chloride into the tertiary  
153 water in accordance with GB1266(GB1266: specifies the configuration of chemical reagent  
154 neutral salt spray solution) and GB6682(GB6682: specifies the water specifications and  
155 experimental methods for the analysis laboratory); and then, test the PH value of the obtained  
156 solution at  $25^\circ\text{C}$  and ensure its PH value is between 6.5 to 7.5 to generate the neutral solution.  
157 After that, the neutral solution is deionized with impedance of  $18\Omega$  and mixed with the NaCl  
158 powder (purity of 99 %) to prepare five different concentrations of salt spray test solutions  
159 (i.e.,  $100\text{mg/L}$ ,  $200\text{mg/L}$ ,  $300\text{mg/L}$ ,  $400\text{mg/L}$ , and  $500\text{mg/L}$  of the NaCl).

160 (3) Perform the gas phase test. Firstly, the  $100\text{mg/L}$  NaCl solution is atomized and tested for 15  
161 days. Then repeat the test using different concentrations to generate 30 membrane electrode  
162 samples in total for characteristics analyses. Lastly, the liquid nitrogen embrittlement is used  
163 to cut the electrode samples into  $1\text{cm} \times 1\text{cm}$  flat section to feed the SEM and EDS equipment.  
164 A Quorum sputter coater is used to pre-treat the samples to ensure accurate elemental  
165 analysis. A field emission electron microscope and an energy dispersive X-ray spectrometer  
166 Smart EDX are used to analyze the CCM of the catalyst coated membranes and the surface  
167 microscopy of the gas diffusion layer (GDL).

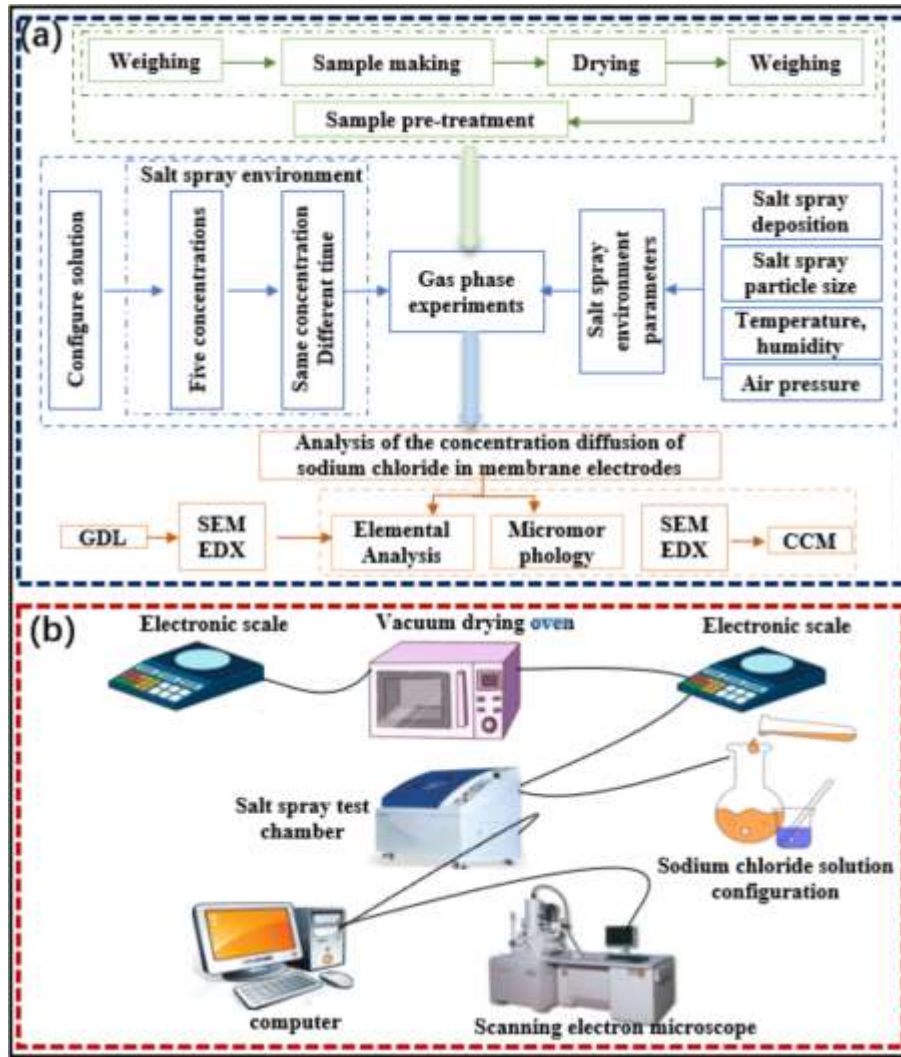


Fig. 1. Overview of experimental test.

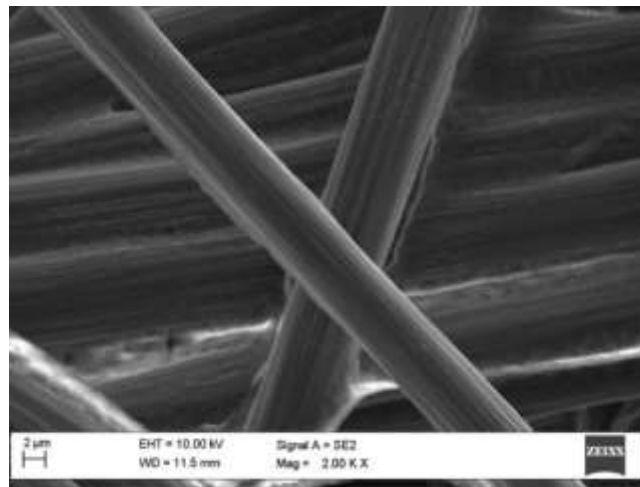
In Fig. 1, the membrane electrodes (platinum loading volume: cathode  $0.3\text{mg}/\text{cm}^2$  & anode  $0.1\text{mg}/\text{cm}^2$ ) are produced by Wuhan Polytechnic New Energy Co. Ltd; the sodium chloride (99% purity) is produced by Tianjin Zhiyuan Chemical Reagent Co. Ltd; the vacuum drying oven (model DZF-6020) and electronic analytical balance (model FA2204) are provided by Shanghai Lichenbangxi Instrument Technology Co. Ltd; the KD-60 standard salt spray chamber is provided by Zhejiang Blue Arrow Instrument Co. Ltd; the German Zeiss field emission electron microscope (model SUPRA 55) and the energy dispersive X-ray spectrometer Smart EDX are used; the Quorum SC7620 sputter coater is supplied by Nanjing Qinshi Technology Co. Ltd.

## 2.2 Microscopic Morphological Characterization

The presence of sodium chloride and its distribution in the membrane electrode are analyzed by a combination of micromorphology and elemental analyses. In order to examine the effect of the

181 experiment time on the surface morphology of the GDL and the microscopic effects of the sodium  
182 chloride diffusion, the membrane electrodes are tested with different periods. In the experimental tests  
183 the crystal formation is made independent of the solution saturation precipitation by setting that the  
184 solution concentration is much lower than the solution saturation points of crystallization  
185 and precipitation. In addition, the experimental impurities are derived from the independent variable  
186 sodium chloride, and the deionized water used for solution preparation has excluded other impurity  
187 components. Therefore, in the experiments the appearance of crystal particles is only from the sodium  
188 chloride in the salt spray environment.

189 The tested results the membrane electrodes with impurities are compared with that without  
190 impurity. Fig. 2 shows SEM surface morphology of the original GDL [28] while Fig. 3 depicts the  
191 GDL morphologies after the sodium chloride experimental tests. Fig. 3 shows the GDL morphologies  
192 with three NaCl mass concentrations (i.e., 300 mg/L, 400 mg/L and 500 mg/L) and six testing periods  
193 (i.e., 24h, 72h, 144h, 216h, 288h, 360h).



194  
195 Fig. 2. SEM surface morphology of original GDL.

196 Comparing Fig. 2 and Fig. 3 one can note that the sodium chloride crystal particles appears in  
197 all the tested GDL morphologies. As the testing time increases, the number of the NaCl crystal  
198 particles significantly increases and the particle distribution changes from sparse to dense quantity.  
199 The most striking feature is that the sodium chloride crystals are uniformly distributed at the carbon  
200 fibers and bonds and the crystal dense increases with time; with different NaCl mass concentrations,  
201 the sodium chloride crystal particles are randomly distributed on the carbon fibers.



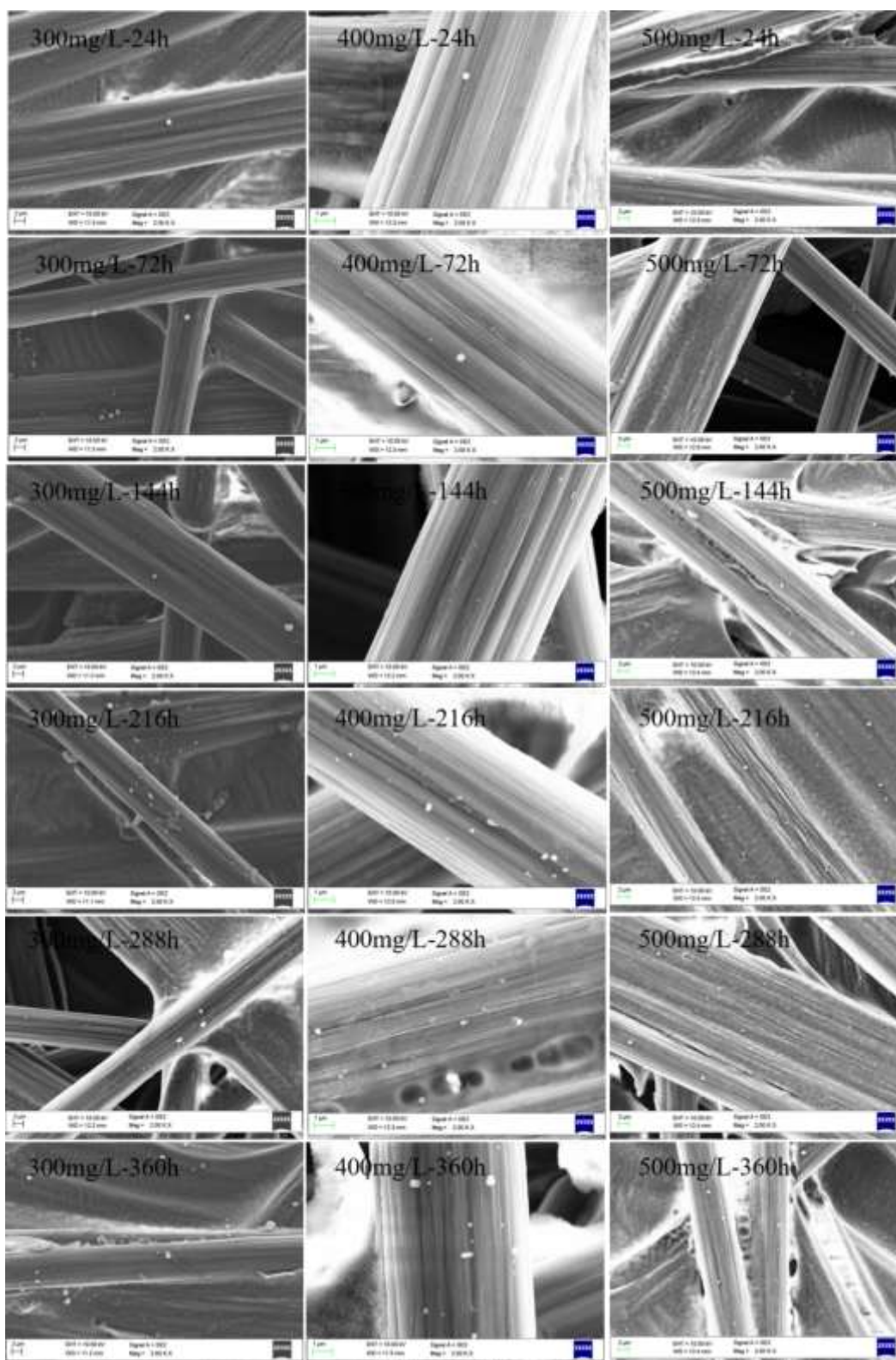
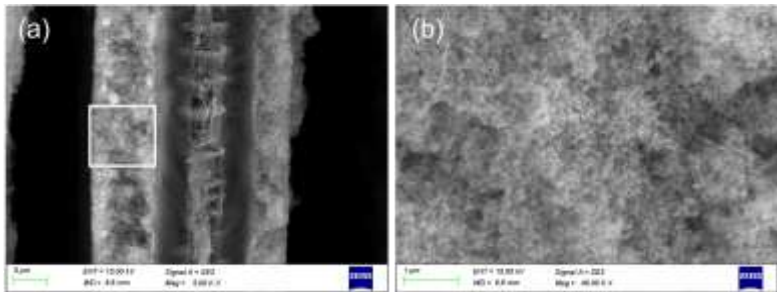


Fig. 3. Surface morphologies of the GDL with different experimental conditions.

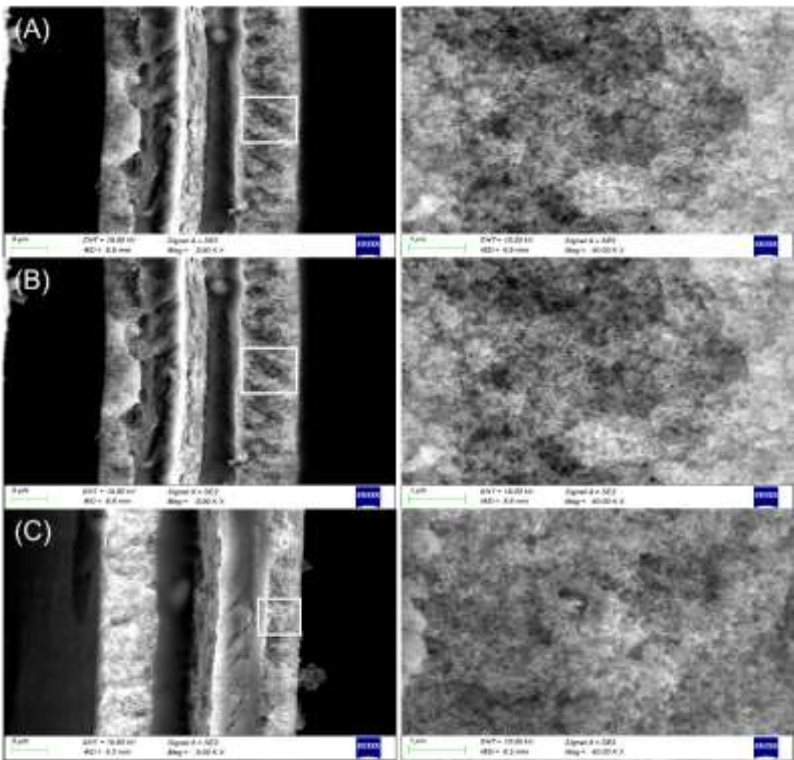
The surface morphologies of the GDLs of the membrane electrodes observed by the electron microscopy demonstrate that the sodium chloride crystal particles are uniformly distributed in the salt spray environment. The overall shape of the crystal particles is regular and shows a typical cubic crystal structure. The distribution of the crystal particles becomes more and more extensive and dense

208 with increasing experimental time at a certain NaCl mass concentration, while the number of crystals  
 209 varies more significantly with different NaCl mass concentrations at a certain testing time.

210 In order to further investigate the concentration dispersion characteristics of the sodium chloride  
 211 at the PEMFC membrane electrodes in the salt spray condition, one testing sample contaminated with  
 212 the sodium chloride is tested for 360h. The base sample is a cross-sectional microstructure of the  
 213 uncontaminated membrane electrode. The cross-sectional microstructures of the CCM layer and the  
 214 membrane electrode and the CCM structure are observed under 15 kV voltage. Fig. 4 manifests the  
 215 cross-sectional microstructure of the original CCM and Fig. 5 depicts the cross-sectional  
 216 microstructure of the tested CCM.



(a) Magnification 5KX (b) Magnification 40KX  
 Fig. 4. Cross-sectional morphology of original CCM.

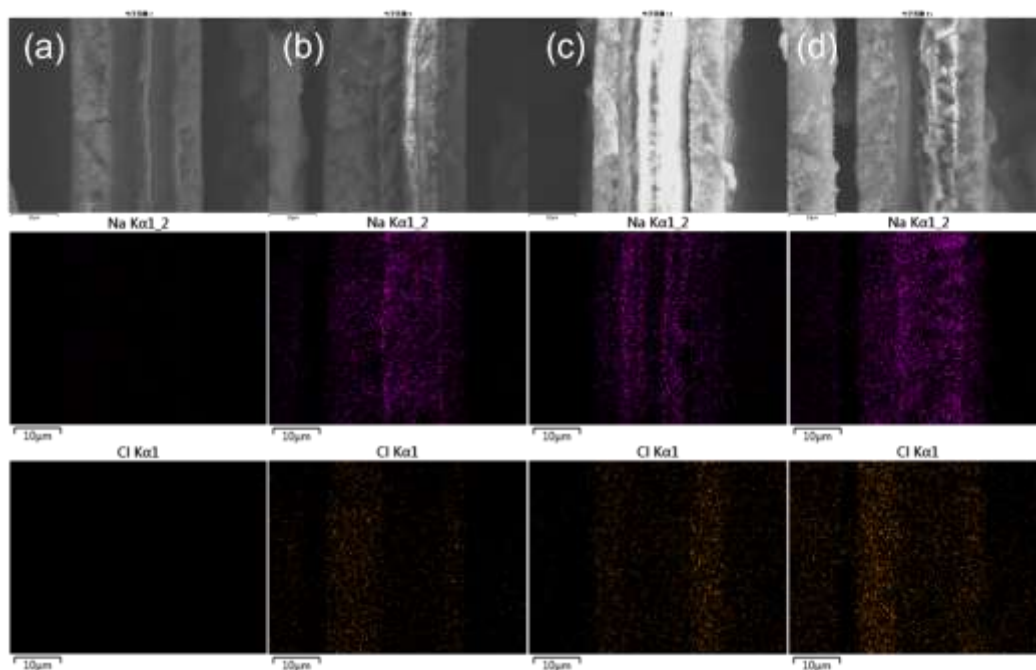


(A) 360h-300mg/L; (B) 360h-400mg/L; (C)360h-500mg/L

Fig. 5. Cross-sectional morphology of tested CCM with five different Cal mass concentrations.

224 As can be seen in Fig. 5, different from the surface morphologies of the GDL in Fig. 3, the  
 225 sodium chloride crystals are not observed. The cross-sectional morphologies do not present any  
 226 crystal attachments at the magnification of both 5 KX and 40 KX; and no crystal structure is found  
 227 after 360h of testing at the concentrations of 300 mg/L, 400 mg/L and 500 mg/L in the salt spray  
 228 environment. It is inferred that the sodium chloride may appear in the catalytic layer and the  
 229 membrane in ionic form. Comparing the CCM surface morphologies before and after the tests in Fig.  
 230 4 and Fig. 5, it can observe that the 360h testing does not cause any visibly morphological changes  
 231 on the microscopic morphology.

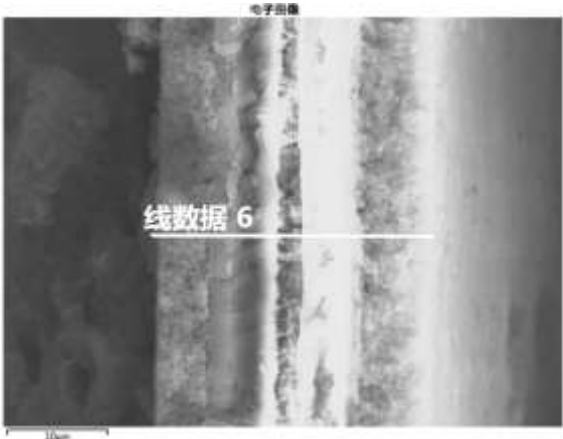
232 Fig. 6 shows the elements and their distributions in the cross sections of the tested membrane  
 233 electrodes. In Fig. 6(a) because the membrane electrode is without any treatment, no sodium or  
 234 chloride elements are found in the elemental distribution. However, the elemental distribution of the  
 235 membrane electrodes tested by the 500 mg/L NaCl mass concentration in a salt spray environment is  
 236 significantly different from Fig. 6(a). The elemental distributions of the sodium and chloride elements  
 237 in Fig. 6(b)-(d) suggest the presence of the sodium in the membrane and the chlorine in the catalytic  
 238 layer. One can note that the sodium and chloride elements are distributed in a homogeneous  
 239 distribution across the proton exchange membrane and catalytic layer; and they are not distributed in  
 240 the same position but in a dispersed manner.



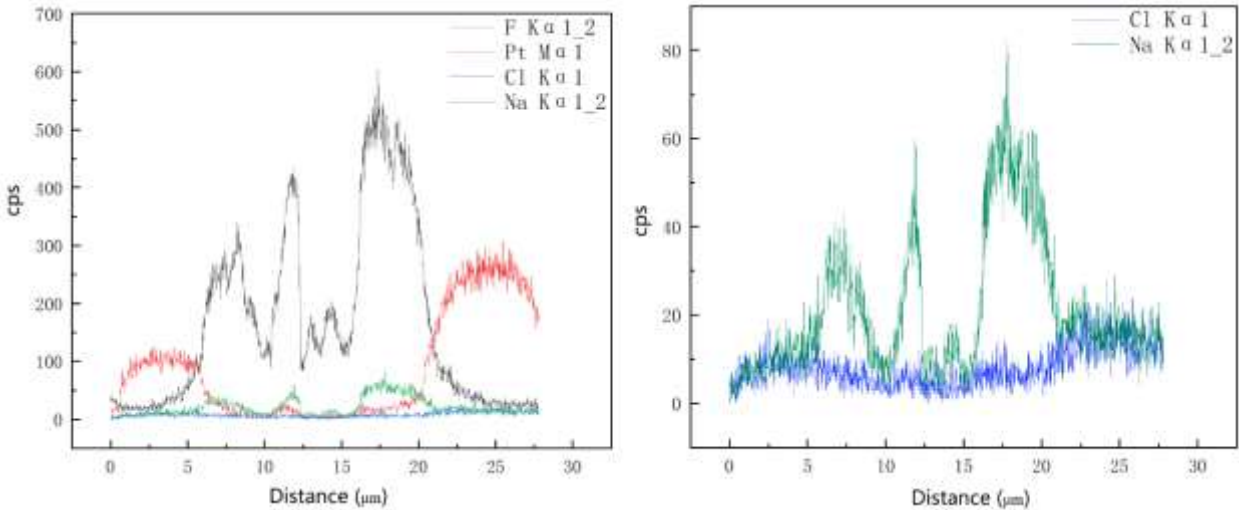
241  
 242 Fig. 6. Elemental distributions of the membrane electrodes: (a) Original membrane electrode; (b)  
 243 membrane electrode tested by 24h; (c)144h; (d) 288h

244 Fig. 6 also suggests that the sodium chloride crystal structure is attached to the GDL, but the  
245 crystal structure is not found on the catalytic layer and the proton exchange membrane. Therefore, it  
246 is clear that the sodium chloride elements appear in two forms: one is the sodium chloride crystal  
247 form on the gas diffusion layer and the other is the ions form on the catalytic and proton exchange  
248 membranes.

249 Fig. 7 depicts the cross-sectional morphology of the CCM after 360h testing in a salt spray  
250 environment with a NaCl mass concentration of 500 mg/L and Fig. 8 shows the elements distribution  
251 curves of the cross section. It can observe that in Fig. 8(a) the element F fluctuates at a distance of 5  
252 to 20  $\mu\text{m}$  and forms three peaks; the element Pt forms two peaks and the peak values are about 100cps  
253 at 2.6 $\mu\text{m}$  and 300cps at 27.5 $\mu\text{m}$ , respectively; the element Cl appears three peaks appear between  
254 5 $\mu\text{m}$  and 22.5 $\mu\text{m}$  with a maximum peak value of about 80cps; and the overall distribution curve of  
255 the element Na is similar to that of the element Cl but with much smaller peaks.



256  
257 Fig. 7. Location of the cross section of the CCM after 360h testing.

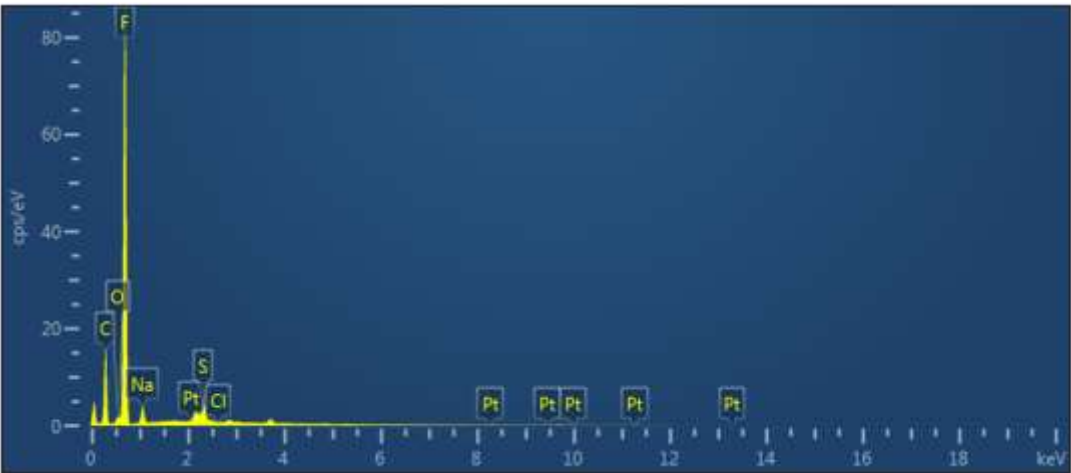
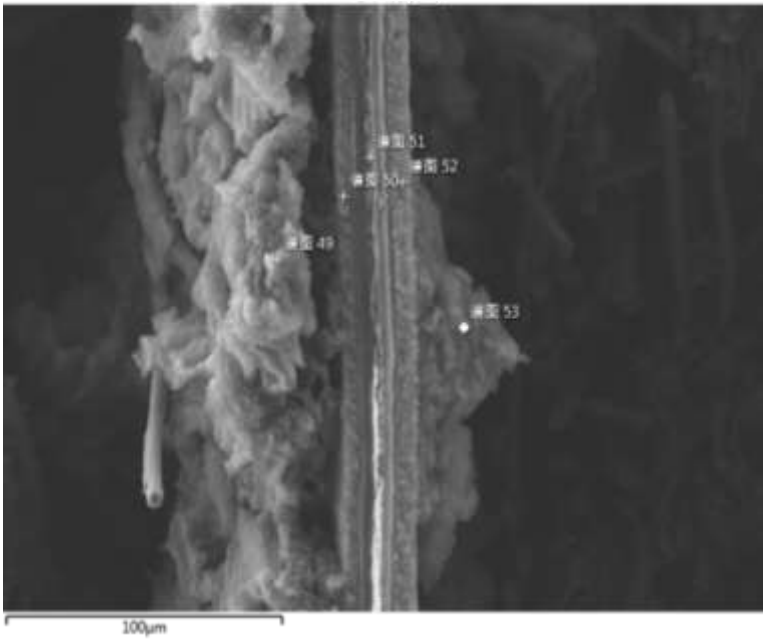


258  
259 Fig. 8. Elements distribution curves of the cross section.

260 **3. Evaluation of Sodium Chlorine Contamination**

261 **3.1. Elements Contents**

262 In the element analysis of the membrane microstructure, in order to detect the relative content  
263 of each element, the element spot analysis method is performed. A sample in 300h-500mg/L condition  
264 is used to interpret the element spot position and element content spectrum, as shown in Fig. 9 and  
265 Table 2. It can be seen that the elements of C, O, Na, Pt, S and Cl are detected. The C and O contents  
266 account for the largest percentages in the GDL, PEM and catalytic layer; followed by the F content;  
267 the content of Na is larger than that of Cl and S.





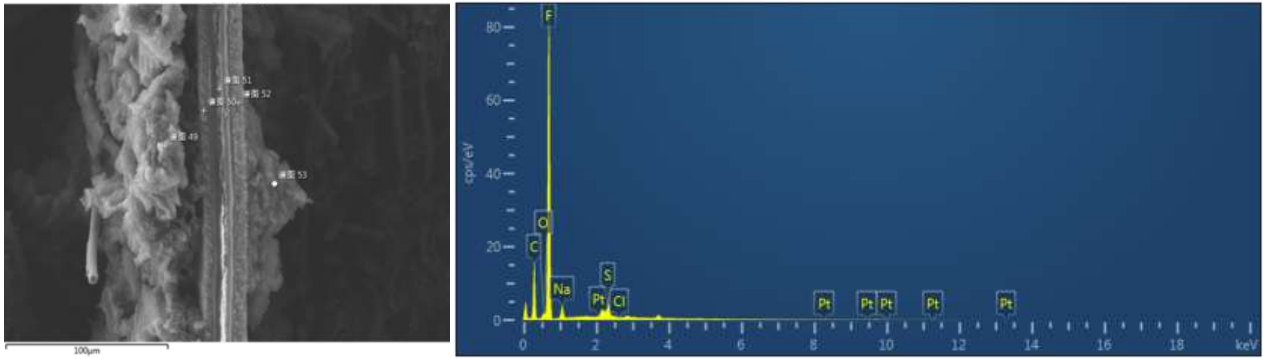


Fig. 9. Energy spectrum of spot analysis in the membrane.

Table 2. Element contents results

	C	F	Pt	Na	Cl	O	S
GDL anode	95.47%	1.20%	0	0.01%	0.01%	3.32%	0%
GDL cathode	93.26%	2.39%	0	0.04%	0.03%	4.29%%	0
PEM	31.53%	61.5%	0	2.92%	0	2.83%	1.21%
Anode of catalytic layer	76.51%	17.22%	1.86%	0.57%	0.08%	3.34%	0.41%
Cathode of catalytic layer	70.16%	17.2%	3.57%	0.52%	0.14%	8.40%	0.01%

Table 3 manifests the elements contents in the membrane with respect to varying time and Table 4 displays the concentration effect. It can be seen that the percentage content of the sodium in the membrane becomes larger with increasing test time and concentration; at 24h-500mg/L testing the sodium percentage content is 0.64% in the membrane and this value increases to 2.92% at 360h-500mg/L testing in Table 3; at 100mg/L-360h testing the sodium percentage content is 1.61% in the membrane and this value increases to 2.92% at 500mg/L-360h testing in Table 4. However, the chlorine content does not show any change rule in the membrane with respect to testing time and solution concentration.

Table 3. Elements percentage contents in time-varying condition

500mg/L	24h	72h	144h	216h	288h	360h
C	32.93%	42.52%	48.67%	46.26%	34.95%	31.53%
F	62.6%	52.9%	44%	48.5%	58%	61.5%
Pt	0.22%	0.05%	0.12%	0	0	0
Na	0.64%	1.3%	1.58%	1.94%	2.45%	2.92%
Cl	0.01%	0	0.05%	0	0	0
O	2.45%	2.16%	5.09%	2.54%	2.44%	2.83%
S	1.16%	1.08%	0.59%	0.75%	1.75%	1.21%

Table 4. Elements percentage contents in different solution concentrations

360h	100mg/L	200mg/L	300mg/L	400mg/L	500mg/L
------	---------	---------	---------	---------	---------

C	38.04%	20.91%	30.11%	31.71%	31.53%
F	56.06%	68.6%	63.07%	62.56%	61.5%
Pt	0.01%	0.08%	0.02%	0.04%	0
Na	1.61%	2.38%	2.56%	2.86%	2.92%
Cl	0.01%	0.03%	0.01%	0.01%	0
O	1.75%	3.38%	2.92%	1.95%	2.83%
S	2.53%	4.62%	1.11%	0.86%	1.21%

### 3.2 Evaluation of Membrane Contamination Degree

The affinity of the membranes is critical to different concentrations of contaminants; and hence, it is important to evaluate the contaminant degree in the membranes. For this purpose, this study adopts two steps to qualify and quantify the contaminant degree. In the first step, qualitative analysis is carried out to qualify the contaminant degree based on the experimental results of the microscopic characterization. In Table 3 and Table 4 one can note that the sodium content in the proton exchange membranes increases with increasing time and solution concentration and the chloride ions are hardly absorbed into the membrane. As a result, the degree of membrane contamination can be evaluated by the sodium content. For this reason, the sodium to fluorine ratio is proposed as an evaluation merit to qualify the membrane contamination. The sodium to fluorine ratio in the membranes measured by the EDX is summarized in Table 5. The EDX results show that as the NaCl mass concentration increases, the absorption of sodium ions in the membranes increases and the sodium to fluorine ratio gradually increases; similarly, the sodium to fluorine ratio in the membranes gradually increases with the increase of the testing time. These observations suggest that the increase of both the testing time and NaCl mass concentration will lead to the increase of the impurity absorption by the membrane and the increase of the sodium to fluorine ratio. As a result, the larger the sodium to fluorine ratio, the heavier the contaminant degree in the membrane.

Table 5. Sodium to fluorine ratio

Testing time	Na/F ratio	NaCl mass concentration	Na/F ratio
24h	$1.02 \times 10^{-2}$	100mg/L	$2.87 \times 10^{-2}$
72h	$2.46 \times 10^{-2}$	200mg/L	$3.47 \times 10^{-2}$
144h	$3.59 \times 10^{-2}$	300mg/L	$4.06 \times 10^{-2}$
216h	$4.00 \times 10^{-2}$	400mg/L	$4.57 \times 10^{-2}$
288h	$4.22 \times 10^{-2}$	500mg/L	$4.75 \times 10^{-2}$
360h	$4.75 \times 10^{-2}$	—	—

In the second step, quantitative analysis is carried out to quantify the contaminant degree by

302 developing a diffusion rate prediction model for sodium contamination in the membrane. The  
 303 prediction model that considers the testing time and NaCl mass concentration factors is expressed in  
 304 Eq. (1) [29].

$$305 \quad W = W_j(C, t) \quad (1)$$

306 where,  $W$  is the membrane contaminant degree,  $W_j$  is a prediction function related to the NaCl mass  
 307 concentration  $C$  and the testing time  $t$  in the salt spray environment.

308 The prediction function can be established by regressing the sodium mass percentage in the  
 309 experimental tests [31-33].

$$310 \quad W_j(C, t) = K_c \cdot K_t \quad (2)$$

311 where  $K_c$  denotes the change rate of the sodium mass percentage with respect to the NaCl mass  
 312 concentration and  $K_t$  denotes the change rate of the sodium mass percentage with respect to time.

313  $K_c$  can be estimated by fitting the experimental data using the least squares method. Fig. 10  
 314 shows the fitting results that describing the relationship between the sodium mass percentage and the  
 315 solution contamination concentrations.

316 Similarly,  $K_t$  can be estimated according to Table 6 using the least squares method. The fitting  
 317 result is shown in Fig. 11.

$$318 \quad k_t = 0.0024 + 3.9244 \times 10^{-6}t \quad (3)$$

319 Combining Eq. (2) and Eq. (3), it yields

$$320 \quad W_j(C, t) = (0.0024 + 3.9244 \times 10^{-6}t) \cdot k_c \quad (4)$$



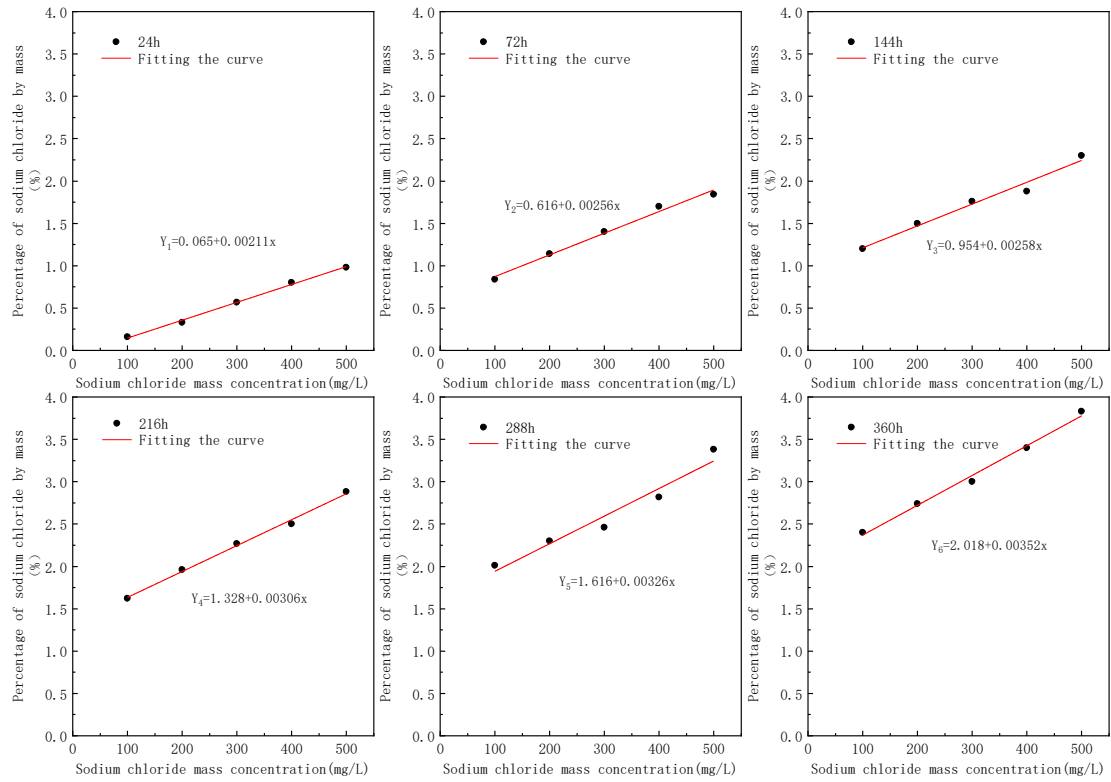


Fig. 10. Fitting curve of sodium mass percentage to concentration

Table 6. Sodium mass percentage in the membrane

	24h	72h	144h	216h	288h	360h
100mg/L	0.16%	0.84%	1.2%	1.62%	2.01%	2.4%
200mg/L	0.33%	1.14%	1.5%	1.96%	2.3%	2.74%
300mg/L	0.57%	1.4%	1.76%	2.27%	2.46%	3.0%
400mg/L	0.8%	1.7%	1.88%	2.5%	2.82%	3.4%
500mg/L	0.98%	1.84%	2.3%	2.88%	3.38%	3.83%

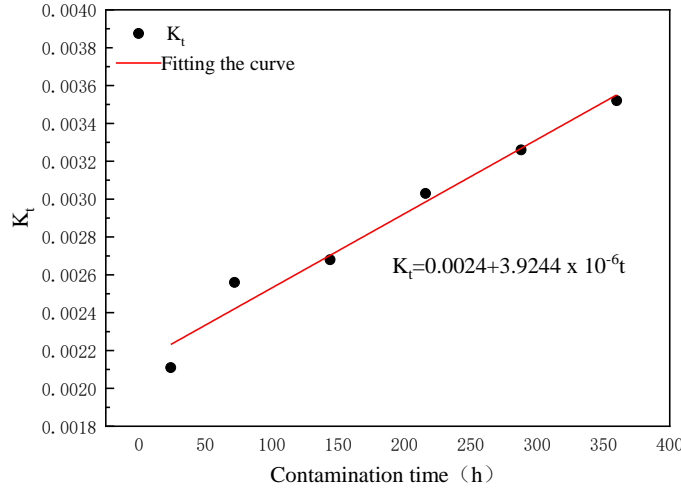


Fig. 11. Fitting curve of the sodium mass percentage to time.

Eq. (4) can be used as an empirical model to predict the sodium mass percentage in the proton exchange membrane. Assuming that the total mass in the test area of the PEMFC membrane electrode remains constant, the relationship between the sodium mass percentage to total element mass can be expressed as

$$W_j = \frac{m_{Na}}{m_{Na} + m} \quad (5)$$

where  $m_{Na}$  is the sodium mass and  $m$  is the total element mass in the test area.

Combining (4) and (5) it obtains

$$m_{Na} = \frac{(0.0024 + 3.9244 \times 10^{-6} t) \cdot k_c}{1 - (0.0024 + 3.9244 \times 10^{-6} t) \cdot k_c} \cdot m \quad (6)$$

If the concentration is determined, the sodium diffusion rate can be obtained according to the principle of partial derivatives.

$$V_{Na} = \frac{d[m_{Na}]}{dt} \quad (7)$$

Combining (6) and (7) the sodium diffusion rate can be rewritten as

$$V_{Na} = \frac{\partial m_{Na}}{\partial t} = \frac{3.9244 \times 10^{-6} k_c m}{[1 - (0.0024 + 3.9244 \times 10^{-6} t) k_c]^2} \quad (8)$$

As a result, the diffusion rate prediction model for sodium in the membrane is obtained to quantify the membrane contamination degree.

## 343 **4. Conclusions**

344 This work experimentally explores the influence of the sodium chloride pollution on the PEMFC  
345 performance in the marine salt spray environment by analyzing the concentration diffusion  
346 characteristics of the sodium chloride in the PEMFC membrane electrodes. The findings of the  
347 experimental results demonstrate that:

348 (1) Sodium chloride appears on the membrane electrode in two ways, as crystals on the gas  
349 diffusion layer structure and as ions on the catalytic layer and the proton exchange membrane  
350 structure. The crystals are uniformly distributed on the carbon fibers of the gas diffusion layer in the  
351 salt spray environment, and the crystal distribution becomes more and more dense with time, but the  
352 crystal particle size does not grow significantly.

353 (2) The effect of sodium chloride on each structure of the membrane electrode is different, and  
354 the percentage content of sodium atoms detected on the proton exchange membrane structure is up to  
355 2.92 %. The atomic percentage content is positively correlated with the experimental time and  
356 concentration. the sodium element distribution curve presents a similar distribution trend to that of  
357 the F element. The overall sodium content is detected to be higher than that of chlorine element.

358 (3) Based on the experimental test result data, a quantitative relationship is established to  
359 evaluate the contamination degree of the membrane electrode. The linear fitting method in the least  
360 squares method is used to propose the relationship between the diffusion rate of sodium elements in  
361 the membrane, the contamination time and the contamination concentration under the salt spray  
362 environment, and to construct a prediction model for the diffusion rate of contaminated ions that can  
363 be used in the actual working conditions under the action of cell operation time and salt spray salt  
364 content.

## 365 **Acknowledgements**

366 The research leading to these results has received funding from the Norwegian Financial  
367 Mechanism 2014-2021 under Project Contract No 2020/37/K/ST8/02748.

## 368 **Conflict of interests**

369 The authors declare that there is no conflict of interests regarding the publication of this article.

370

371 **Research Data**

372 All the data can be requested from the corresponding author.

373

374 **References**

- 375 [1] ZHANG G, YANG G, LI S, et al. Molecular dynamics study on the impacts of cations in sea salt  
376 aerosol on transport performance of Nafion Membranes for PEMFCs in marine application [J].  
377 International Journal of Hydrogen Energy, 2022, 47(63): 27139-27149.
- 378 [2] Wen Xiaofei, Zhou Shengnan, Zhan Zhigang, et al. Equivalent ohmic polarization model for  
379 PEMFC based on sodium chloride poisoning [J]. Journal of Power Sources, 2021, 45: 744-  
380 746+785.
- 381 [3] Mikkola M. S, Rockward T, Uribe F. A, et al. The Effect of NaCl in the Cathode Air Stream on  
382 PEMFC Performance[J]. Fuel Cells, 2006, 7(2):153-158.
- 383 [4] Unnikrishnan A, Janardhanan V M, Rajalakshmi N, et al. C hlorine-contaminated anode and  
384 cathode PEMFC-recovery perspective[J]. Journal of Solid-State Electrochemistry, 2018,  
385 (22):2107-2113
- 386 [5] B. Shabania, M. Hafttananian, Sh. Khamani, et al. Poisoning of proton exchange membrane fuel  
387 cells by contaminants and impurities: Review of mechanisms, effects, and mitigation strategies[J].  
388 Journal of Power Sources, 2019, 427:21-48.
- 389 [6] Md. Aman Uddin, Xiaofeng Wang, Jing Qi, et al. Effect of Chloride on PEFCs in Presence of  
390 Various Cations[J]. Journal of The Electrochemical Society, 2015, 162(4): F373-F379.
- 391 [7] Wang Leilei, He Gaohong, Jie Xiao, et al. Effect of metal ions on the performance of proton  
392 exchange membranefuel cell [J]. Power Technology, 2007(03):205-208.
- 393 [8] Jie X, Hou JB, Shao ZG, et al. Effect of impurity  $\text{Na}^+$  on Pt/C gas-diffusion electrode in PEMFC  
394 [J]. Power Technology, 2009, 33(03):175-177.
- 395 [9] Strmcnik D, Vliet D F, Chang K C, et al. Effects of  $\text{Li}^+$ ,  $\text{K}^+$  and  $\text{Ba}^{2+}$  Cations on the ORR at  
396 Model and High Surface Area Pt and Au Surfaces in Alkaline Solutions[J]. The Journal of  
397 Physical Chemistry Letters, 2011, 2(21):2733-2736.
- 398 [10] Jayasayee K, Veen JARV, Hensen E, et al. Influence of chloride ions on the stability of PtNi  
399 alloys for PEMFC cathode[J]. Electrochemical Acta, 2011, 56(20):7235-7242.
- 400 [11] Uddin M A, Wang X, Qi J, et al. Effect of Chloride on PEFCs in Presence of Various Cations[J].  
401 Journal of the Electrochemical Society, 2015, 162(4): F373-F379.

- 402 [12]Arruda T, Shyam B. Investigation into the competitive and site-specific nature of anion  
403 adsorption on Pt using in situ X-ray. 2008, 508(1-2):41-47.
- 404 [13]MO J, STEEN S, KANG Z, et al. Study on corrosion migrations within catalyst-coated  
405 membranes of proton exchange membrane electrolyzer cells [J]. International Journal of  
406 Hydrogen Energy, 2017, 42(44): 27343-27349.
- 407 [14]Gutleben H, Bechtold E. Adsorption of chlorine on the Pt(100) face: structural aspects and  
408 desorption kinetics[J]. Surface Science, 1990, 236(3):313-324.
- 409 [15]Ghassemadeh L, Marrony M, Barrera Image, et al. Chemical degradation of proton conducting  
410 perflurosulfonic acid ionomer membranes studied by solid-state nuCclear magnetic resonance  
411 spectroscopy [J]. Journal of Power Sources. 2009, 186(2):334-338.
- 412 [16]Borup R, Meyers J, Pivovar B, et al. Scientific aspects of polymer electrolyte fuel cell durability  
413 and degradation[J]. Chem Rev, 2007, 107(10):3904-3951.
- 414 [17] Hori H, Murayama M, Sano T, et al. Decomposition of perfluorinated ion-exchange membrane  
415 to fluoride Ions using zerovalent metals in subcritical water[J]. Industrial & Engineering  
416 Chemistry Research, 2010, 49(2):464-471.
- 417 [18]ZHANG Shuo-shuo, WANG Jie, MA Xiao-juan, et al. Study on the preparation and chemical  
418 degradation mechanism of perfluorinated proton reinforced membrane for fuel cells [J].  
419 Membrane Science and Technology,2020,40(05):39-46.
- 420 [19]Kelly M J, Fafilek G, Besenhard J O, et al. Contaminant absorption and conductivity in polymer  
421 electrolyte membranes[J]. Journal of Power Sources, 2005, 145:249-252.
- 422 [20]Inaba M, Kinumoto T, Kiriake M, et al. Gas crossover and membrane degradation in polymer  
423 electrolyte fuel cells[J]. Electrochimica Acta, 2006, 51(26):5746-5753.
- 424 [21]Liu W, Zuckerbrod D. In situ detection of hydrogen peroxide in PEM fuel cells[J]. Journal of The  
425 Electrochemical Society, 2005, 152(6): A1165-A1170.
- 426 [22]B. Kienitz, H. Baskaran, T. Zawodzinski, Jr, et al. A Half Cell Model of Steady State PEM Fuel  
427 Cell Performance Degradation under Contamination by Foreign Cationic Species[J]. ECS  
428 Transactions, 2007, 11(1):777–788.
- 429 [23]Jing Xie, Shuai Ban, Bei Liu, et al. A molecular simulation study of chemical degradation and  
430 mechanical deformation of hydrated Nafion membranes[J]. Applied Surface Science.2016,

362:441-447.

[24] UDDIN M A, PARK J, BONVILLE L, et al. Effect of hydrophobicity of gas diffusion layer in calcium cation contamination in polymer electrolyte fuel cells [J]. *International Journal of Hydrogen Energy*, 2016, 41(33): 14909-14916.

[25] Zhu Minghe. Study on Crystal Habit Control and Caking of Sodium Chloride [D]. Tianjin University, 2018.

[26] GB/T 2423.18-2021, environmental tests-Part 2: Test method Test Kb: salt spray, alternating (sodium chloride solution)[S].

[27] IEC 60068-2-52-1996, Environmental tests -- Part 2-52: Test test Kb: Cyclic salt spray (sodium chloride solution)[S].

[28] Zhou Shengnan. Experimental Study of Sodium Chloride Concentration Diffusion in Ship PEMFC Membrane Electrodes [D]; Zhejiang Ocean University, 2022.

[29] SCIAZKO A, KOMATSU Y, BRUS G, et al. A novel approach to improve the mathematical modelling of the internal reforming process for solid oxide fuel cells using the orthogonal least squares method [J]. *International Journal of Hydrogen Energy*, 2014, 39(29): 16372-16389.

[30] Dohare, I., Singh, K., Pansera, B. A., Ahmadian, A., & Ferrara, M. (2022). Modified sailfish optimization for energy efficient data transmission in IOT based sensor network. *Annals of Operations Research*, 1-31.

[31] Umer, R., Touqeer, M., Omar, A. H., Ahmadian, A., Salahshour, S., & Ferrara, M. (2021). Selection of solar tracking system using extended TOPSIS technique with interval type-2 pythagorean fuzzy numbers. *Optimization and Engineering*, 22, 2205-2231.

[32] Touqeer, M., Umer, R., Ahmadian, A., Salahshour, S., & Ferrara, M. (2021). An optimal solution of energy scheduling problem based on chance-constraint programming model using Interval-valued neutrosophic constraints. *Optimization and Engineering*, 1-29.